Regulation of Lipid-Droplet Transport by the Perilipin Homolog LSD2

Michael A. Welte, Silvia Cermelli, John Griner, Arturo Viera, Yi Guo, Dae-Hwan Kim, Joseph G. Gindhart, and Steven P. Gross

Supplemental Experimental Procedures

Two-Dimensional Electrophoresis

Two-dimensional electrophoresis was performed in two ways. For Figure 1, the method of O'Farrell [S1] was used by Kendrick Labs (Madison, WI). The spot of interest was excised from Coomassie-blue-stained gels and identified by mass spectrometry fingerprinting at the Protein Chemistry Core Facility, Columbia University.

For Figure 6, 2D gel electrophoresis was performed in the Gross laboratory according to standard procedures: 125 μg proteins were precipitated with ReadyPrep 2D Cleanup kits (Bio-Rad) and solubilized in 8 M urea, 2% CHAPS, 50 mM DTT, 0.2% Bio-Lyte 3/10 ampholyte, and 0.002% bromophenol blue. Isoelectric focusing was performed with immobilized pH gradient (IPG) strips (nonlinear pH range from 3–10; Bio-Rad). The dry strips were actively rehydrated with the solubilized protein sample for 12 hr and were electrophoresed for 5.5 hr with IPGphor (Amersham-Pharmacia). The second dimension was run on 8%–16% or 4%–15% polyacrylamide SDS gels with Criterion cells (Bio-Rad).

Phosphatase Treatment

Sixty-five micrograms of total droplet proteins in NP40 lysis buffer was incubated at 37°C for 3 hr with 60 U of calf intestine alkaline phosphatase (Sigma) in a phosphatase reaction buffer (50 μl total reaction volume) and then processed for 2D gel analysis. Phosphatase treatment converted all the spots of lower IEP to a single spot at IEP 8.5 (Figure 6C), suggesting that all LSD2 isoforms visible by 2D Western analysis are due to phosphorylation. We should note that there is an additional variable spot sometimes visible at the very edge of the gel (at an IEP of approximately 8.8); for example, it is present in Figures 6B and 6E but absent in Figure 6C. We are not certain if this spot is a gel artifact or represents an additional modification such as esterification.

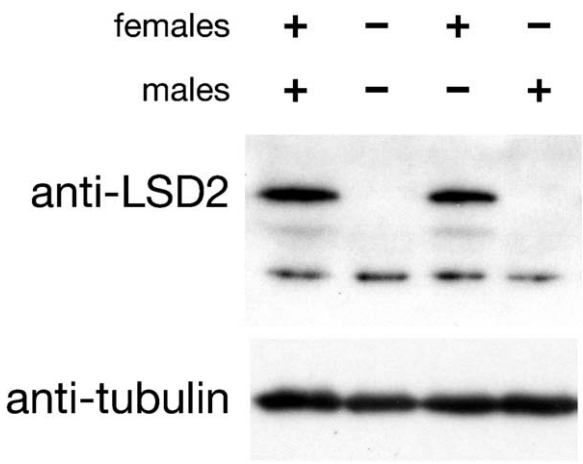

Figure S1. LSD2 Protein Is Maternally Contributed to Embryos

Wild-type (+) and *LSD2*^{KG} mutant (−) parents were crossed to each other in all possible combinations. Embryos derived from these crosses were collected and analyzed by Western blotting as in Figure 2B. LSD2 protein was detected only if the mothers were wild-type. Thus, like lipid droplets, LSD2 protein is maternally provided, and the zygotic contribution appears negligible.

Immunoblot Analysis

After SDS-PAGE or 2D gel electrophoresis, proteins were electrotransferred to PVDF membranes. Membranes were incubated with anti-LSD2 (dilution 1:5000 or 1:20000) and then peroxidase-conjugated donkey or goat anti-(rabbit IgG) antibodies (dilution 1:10000). The ECL Western blotting detection system (PerkinElmer) was used for visualization. Membranes were either stained with Amido black or probed with an anti-α tubulin antibody (T-5168, Sigma) to assess equal loading on 1D gels.

Fly Stocks and Cultured Cells

Oregon-R was the wild-type stock. We used the Δ(*halo*) strain [S2] to generate embryos deleted for *halo*. Two P element insertions into *LSD2* have been described: KG00149 [S3] and BG00016 [S4]. We generated *LSD2* alleles *Δ1* and *Δ2* from insertion KG00149 by P transposase-mediated excision of the P element with standard procedures. *Df(1)RK3* and *Df(1)RK4* are large chromosomal deletions with proximal breakpoints that map cytologically in the general vicinity of *LSD2*. With PCR primers surrounding the P insertion site of *LSD2*^{KG}, we were able to consistently amplify fragments of wild-type size from genomic DNA of wild-type and *Df(1)RK3/LSD2*^{KG} flies, but not from *LSD2*^{KG}/*LSD2*^{KG} and *Df(1)RK4/ LSD2*^{KG} flies. We conclude that the *LSD2* gene is deleted in *Df(1)RK4* but not *Df(1)RK3*, consistent with the Western data in Figure 2B. Unless otherwise noted, the analysis of *LSD2* mutants employed allele *LSD2*^{KG}. For isolation of lipid droplets from cultured cells, we used the permanent cell lines S2 and S3, derived from wild-type embryos [S5].

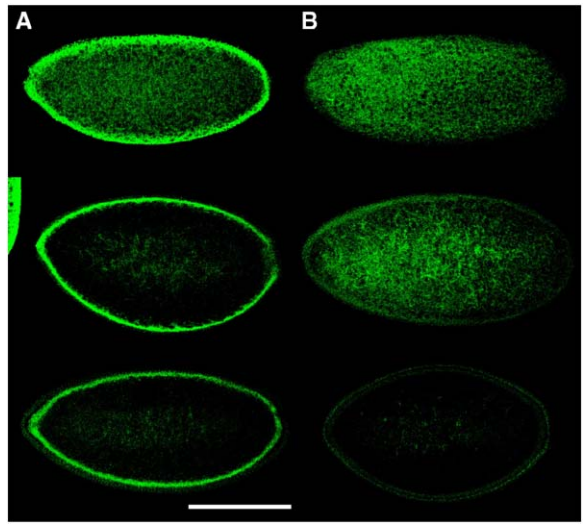

Figure S2. LSD2 Is Present in the Embryo Periphery

Embryos of various genotypes were immunostained with the LSD2 antibody to detect the intracellular distribution of LSD2.

(A and B) Wild-type (A) and *LSD2*^{KG} (B) embryos in phase 0 (top), phase I (middle), or phase II (bottom). The antibody gives some background staining in mutant embryos; comparison with the wild-type shows that in all phases, LSD2 is present in the embryo periphery, where lipid droplets are located. The scale bar represents 200 μm.

Immunostaining

For LSD2 immunostaining, embryos were fixed in 0.9% formaldehyde for 10 min before vitelline membranes were removed by heptane-methanol treatment. Embryos were stored at –20°C overnight in methanol. Anti-LSD2 (1:500–1:1000) was followed by incubations with mouse anti-rabbit and Alexa488-conjugated goat anti-mouse antibodies (at 1:1000 each). Because in whole mounts this antibody gave good signal only under conditions that extract neutral lipid, we could not directly test for colocalization of LSD2 and neutral lipids within embryos. When embryos were broken to disperse embryonic organelles and then fixed under conditions that do not extract lipids, it was possible to detect LSD2 by antibody staining. Embryos were centrifuged before fixation to determine whether LSD2 was physically associated with lipid droplets [S6]. Lipid droplets, yolk vesicles, and Golgi were visualized as described [S2]. DNA was labeled by Hoechst 33258. Embryos were squashed into buffer and processed essentially as previously described [S7] with Nile red to label lipid droplets and anti-Cdic (Chemicon) or anti-LSD2, respectively, to detect dynein or LSD2 on lipid droplets. Because intensity of dynein signal varies across single preparations, we did not attempt to quantify the occurrence of dots between the two genotypes, but relied on Westerns (Figure 4G) instead. Confocal images in Figure 3 and Figures 4D–4F and 4H were acquired on a Leica TCS SP2 confocal microscope.

Particle Tracking and Analysis

In the wild-type, embryonic droplets have a characteristic appearance by differential interference contrast (DIC) videomicroscopy and can be easily distinguished from the other organelles, such as yolk vesicles and mitochondria, in a similar size class [S8]. This was also true for lipid droplets in *LSD2*^{KG} embryos. Embryos were flattened into halocarbon oil, and video-enhanced DIC recordings of moving droplets were made onto videotape. The location of individual droplets as a function of time was determined with nanometer-level resolution with centroid analysis. Particle tracking and analysis was done as described previously [S7]. Histograms of run lengths were fit to the sum of two decaying exponentials to characterize the properties of the short-slow and long-fast travel states. Absolute values of specific parameters can be influenced by the choice of which droplets are tracked; to ensure meaningful comparisons, the data in Table 1 are all new, and tracking and analysis of the motion in the wild-type and mutant backgrounds were done in parallel by the same person.

Yeast Two-Hybrid Screen

The LD domain of Klar [S6] was cloned into the bait vector pEG202 [S9]. The pEG-Klar-LD fusion protein was used to screen the RFLY1 *Drosophila* embryonic cDNA library as described previously [S10]. Putative Klar-LD interactors were characterized by PCR amplification with primers BCO1 and BCO2 [S11]. Full-length LSD2 was cloned into the prey vector pJG4-5 [S9]. Putative interactors were retested for enhancement of *LEU2* and *lacZ* reporter-gene expression (detected by growth in the absence of leucine or by Xgal staining, respectively) in a bait- and prey-dependent manner with yeast strain EGY48 [S11].

Supplemental References

S1. O'Farrell, P.H. (1975). High resolution two-dimensional electrophoresis of proteins. J. Biol. Chem. 250, 4007–4021.

S2. Gross, S.P., Guo, Y., Martinez, J.E., and Welte, M.A. (2003). A determinant for directionality of organelle transport in *Drosophila* embryos. Curr. Biol. *13*, 1660–1668.

S3. Grönke, S., Beller, M., Fellert, S., Ramakrishnan, H., Jackle, H., and Kuhnlein, R.P. (2003). Control of fat storage by a *Drosophila* PAT domain protein. Curr. Biol. *13*, 603–606.

S4. Teixeira, L., Rabouille, C., Rorth, P., Ephrussi, A., and Vanzo, N.F. (2003). Drosophila Perilipin/ADRP homologue Lsd2 regulates lipid metabolism. Mech. Dev. *120*, 1071–1081.

S5. Schneider, I., and Blumenthal, A. (1978). *Drosophila* cell and tissue culture. In Biology and Genetics of *Drosophila*, Volume 2B, M. Ashburner and T.R.F. Wright, eds. (New York: Academic Press), pp. 266–315.

S6. Guo, Y., Jangi, S., and Welte, M.A. (2005). Organelle-specific control of intracellular transport: Distinctly targeted isoforms of the regulator Klar. Mol. Biol. Cell *16*, 1406–1416.

S7. Gross, S.P., Welte, M.A., Block, S.M., and Wieschaus, E.F. (2000). Dynein-mediated cargo transport in vivo. A switch controls travel distance. J. Cell Biol. *148*, 945–956.

S8. Welte, M.A., Gross, S.P., Postner, M., Block, S.M., and Wieschaus, E.F. (1998). Developmental regulation of vesicle transport in *Drosophila* embryos: Forces and kinetics. Cell *92*, 547–557.

S9. Zervos, A.S., Gyuris, J., and Brent, R. (1993). Mxi1, a protein that specifically interacts with Max to bind Myc-Max recognition sites. Cell *72*, 223–232.

S10. Gindhart, J.G., Chen, J., Faulkner, M., Gandhi, R., Doerner, K., Wisniewski, T., and Nandlestadt, A. (2003). The kinesin-associated protein UNC-76 is required for axonal transport in the Drosophila nervous system. Mol. Biol. Cell *14*, 3356–3365.

S11. Ausubel, F.M., Brent, R., Kingston, R.E., Moore, D.D., Seidman, J.G., Smith, J.A., and Struhl, K. (1997). Current Protocols in Molecular Biology (New York: John Wiley and Sons).